Evaluation of digital photogrammetric aerial camerasystems

Radiometric Evaluation of DMC, ADS 40 and Ultracam X

THOMAS HANUSCH[1] & EMMANUEL BALTSAVIAS[2]

Abstract:
As a member of the evaluation team for radiometric analysis in the DGPF Project "Evaluierung digitaler photogrammetrischer Luftbildkamerasysteme", we will present the first results of our investigations.

The following points were investigated:

- *Histogram analysis*
- *Detection of artifacts, e.g. saturation, blooming, interlacing, compression*
- *Analysis of the vignetting effects*
- *Noise analysis*
- *Linearity of the sensor*

All investigations are performed in the spectral and panchromatic channels, using 16-bit. When the raw images were available, this data was used too.

1 Introduction

This report, presents the first results of our investigations regarding the radiometric analysis of three aerial cameras: DMC, ADS 40 and UltraCamX. First, we show the histogram analysis, followed by the detection of artifacts in the image dataset. We present the results of the sensor linearity analysis using a continuous grey wedge. In addition, visual inspection to detect vignetting effects is performed. The report concludes with an investigation regarding the noise behavior of the sensors. To discuss our results, we are in contact with the camera manufacturers. Up to now, we have contacted Leica Geosystems and Intergraph and have received some explanations from Leica.

2 Data analysis

To analyze the different datasets we worked only in the original 16 bit radiometric range, since a transformation into the 8 bit range would influence the radiometric analysis. All images were saved as 16-bit, but the real number of bits was known only for DMC (12-bit). Based on maximum histogram values, ADS40 appears to be really 16-bit, while UltraCamX images are at

1) Thomas Hanusch, Swiss Ferderal Institute of Technology Zurich, Institute for Geodesy and Photogrammetry, Wolfgang Pauli Strasse 15, 8093 Zurich, Switzerland, E-Mail: hanuscht@geod.baug.ethz.ch
2) Emmanual Baltsavias, Swiss Ferderal Institute of Technology Zurich, Institute for Geodesy and Photogrammetry, Wolfgang Pauli Strasse 15, 8093 Zurich, Switzerland, E-Mail: manos@geod.baug.ethz.ch

least 15-bit. It is not known whether image compression has been performed in the sensor, although the UltraCamX and DMC images were delivered as uncompressed TIFF. Later, it came out that most ADS40 images were compressed (details below). It should be noted that only the ADS40 images were raw (level 0), the others were preprocessed with unknown methods, which make an objective radiometric analysis difficult. For ADS40, also rectified (level 1) images were available. For DMC, the images included panchromatic (after stitching the four DMC subimages together) and the original spectral images. For UltraCamX, the panchromatic (after stitching the nine subimages, called level 2), the spectral images and pansharpened images (level 3). For all three cameras, images from a geometry flight block and a radiometry flight block were available.

2.1 Histogram analysis

2.1.1 DMC

Fig. 1 shows the histogram of the panchromatic channel of the DMC image 10040081 (geometry block). The effective dynamic range is 1600-1800 grey values.

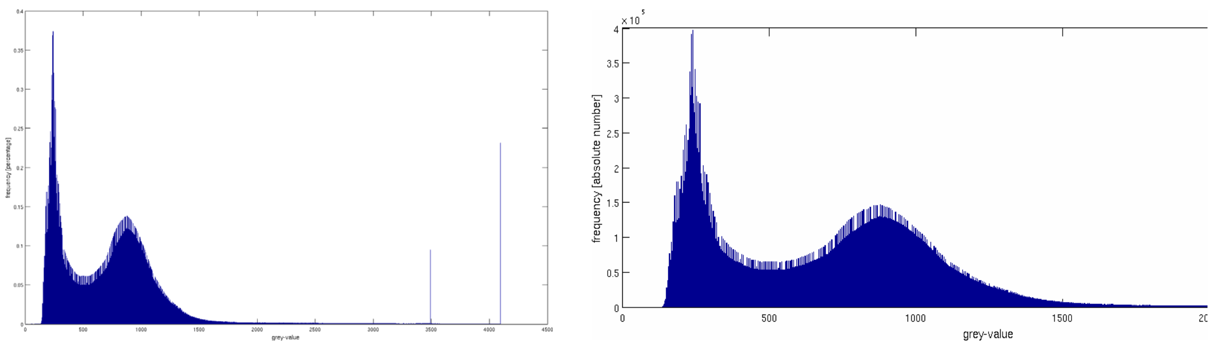

Full histogram

Histogram after cutting off the lowest and highest grey values with less than 0.001% frequency (without histogram stretch)

Fig. 1: Histogram of the panchromatic image 10040081 of the DMC.

Visible are two high peaks at grey values 3491 and 4095 of the diagram (Fig. 1 left), the latter peak representing saturation. In addition, Fig. 1 shows peaks, visible over the whole histogram, with a distance of 6 grey values from one to the next. The reason for this is not clear until now. Fig. 2 shows the histograms of the different channels R, G, B and NIR.

The histogram does not show the peaks every 6 grey values in any channel. The number of overexposed pixels is in case of the green channel very high, see peak at grey value 4095. The peak at grey value 3491 is not visible in the RGB NIR data. The effective grey value range covered is about 1400 to 1700, except for the NIR which has a larger dynamic range (the dynamic range increases from B to G/R to NIR).

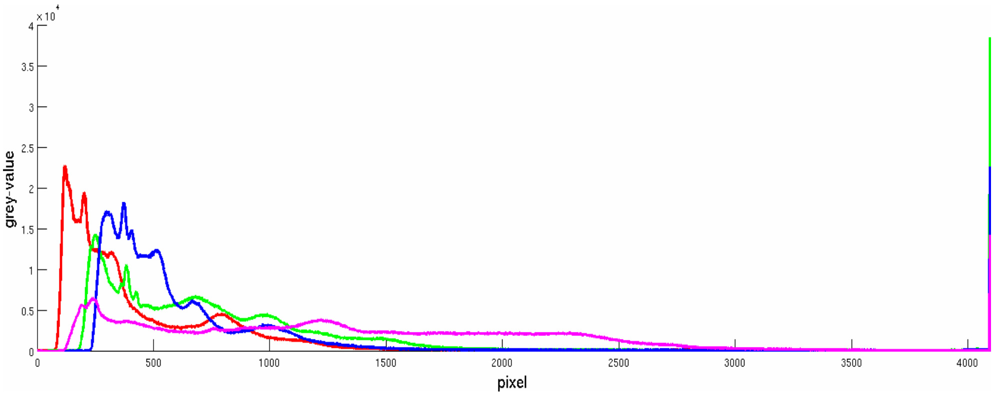

Fig. 2: Histogram of the RBGNIR 10040081 of DMC (RGB, NIR=magenta).

2.1.2 ADS 40

Fig. 3 shows the histogram of the panchromatic channel of the image 1012 of the geometry block (raw images). The effective grey value range covered is about 22,000.

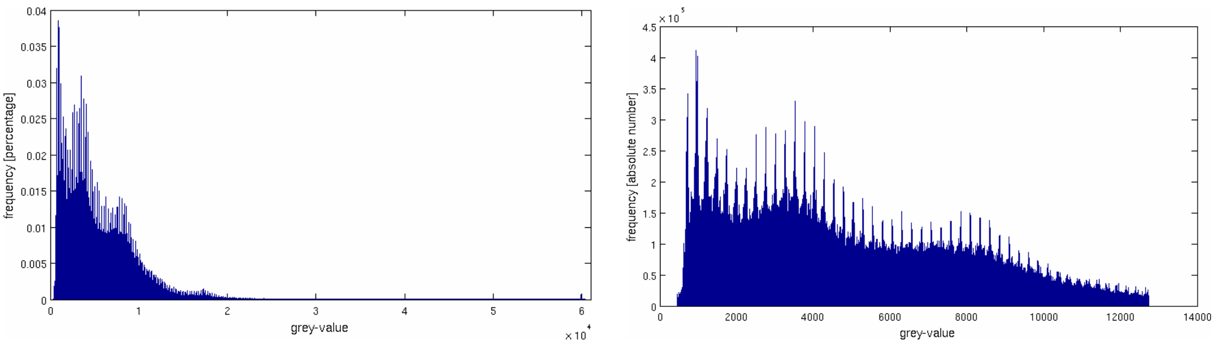

Full histogram

Zoom in

Fig. 3: ADS, panchromatic, image 1012, raw.

Especially, the right graph shows a repetitive structure. The distance between the peaks is 255 grey values (2^8). Fig. 4 shows the equivalent diagram for the RGB and IR image in one graph. The effective dynamic range as with DMC increases from B to G to R to NIR, with a range of 2,500 to 3,500 for RGB and about 7,000 for the NIR. Unlike DMC, the spectral channels have a much lower dynamic range than the panchromatic one. A possible reason is the optical system used for splitting the optical rays into the four spectral components, thus resulting in less energy for each one of them.

The figure shows repetitive structures (peaks), especially in the NIR channel (magenta).

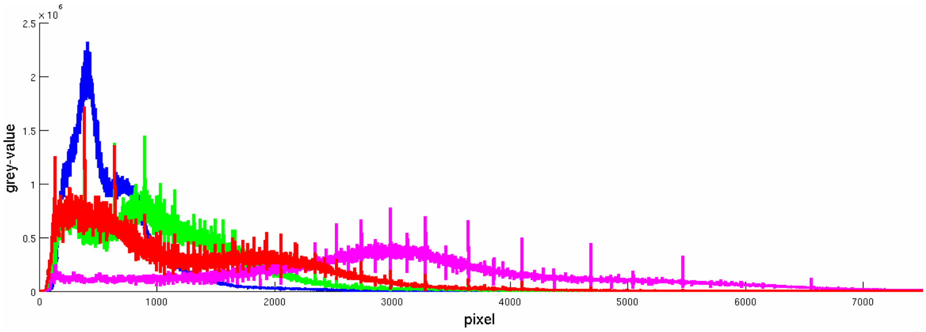

Fig. 4: Histogram, ADS, RGB IR, image 1012, RAW data.

Figure 5 shows the histogram of the same ADS40 image, but rectified (Level 1). Strangely, the dynamic range is much lower than the one of the corresponding raw image (Fig. 3).

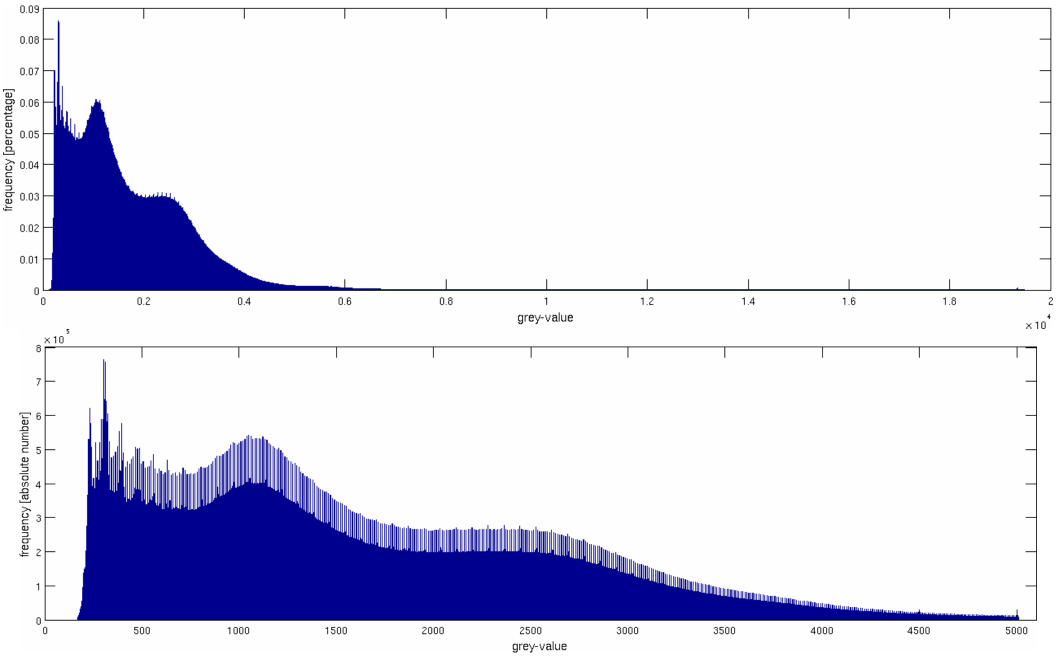

Fig. 5: Histogram ADS, image 1012, panchromatic, after rectification (top: histogram, bottom: zoom in).

The frequent structure (peaks every 2^8 grey values) is caused by a compressing of the data during the flight of the geometry block. According to Leica Geosystems, the compression is lossy. It uses as affine transformation to transform the original data in to the 8 bit range. The affine transformation adapts locally to the grey values and can change every 8 lines. During the decompression the original range of 2^{12} grey values is recovered. During this procedure the original grey values are lost. The method of decompression is unknown, but it is not a linear stretch, otherwise only every 256th grey value would be represented in the histogram.
Fig. 6 shows the result for the radiometry block. On the left side, the histogram of the green channel does not show this peak effect. This applies to all the color channels. On the right side, one of the panchromatic channels is displayed. Here, the compression is applied again. This compression affects both geometry and radiometry block for all panchromatic line CCDs, and

both raw and rectified images. It also affects the spectral images of the geometry block. The spectral channels of the radiometry block according to Leica are not compressed. The dynamic range is as for the geometry block, with the spectral images having again a much lower dynamic range than the panchromatic ones.

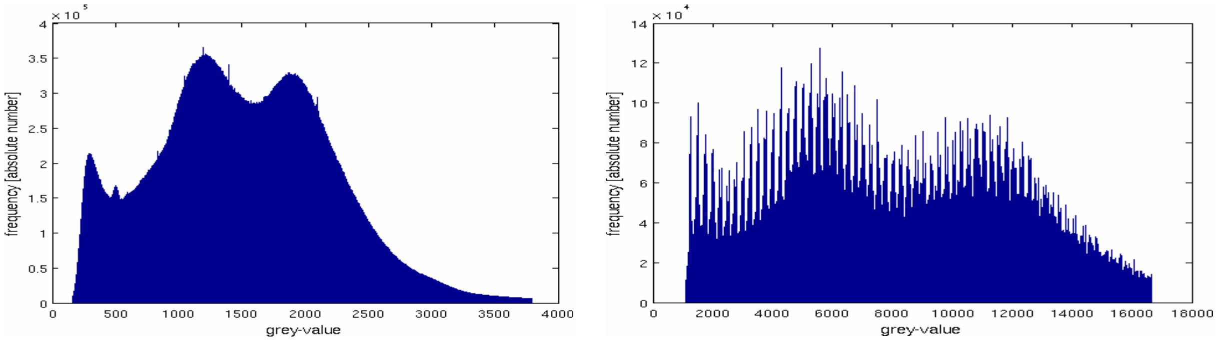

Green channel (nadir) Panchromatic (backward 14°)

Fig. 6: ADS 40, image 1035 (radiometric stripe). Both histograms have been cut-off at left and right borders to allow a zoom-in.

2.1.3 UltraCamX

Fig. 7 shows the histograms for the UltraCamX image 10231067 (radiometry dataset). The histogram does not show any peaks pattern. For panchromatic the effective dynamic range is about 1500 grey values. The dynamic range increases from B to G to R to NIR, the latter having the double range (2800 grey values) compared to the RGB channels.

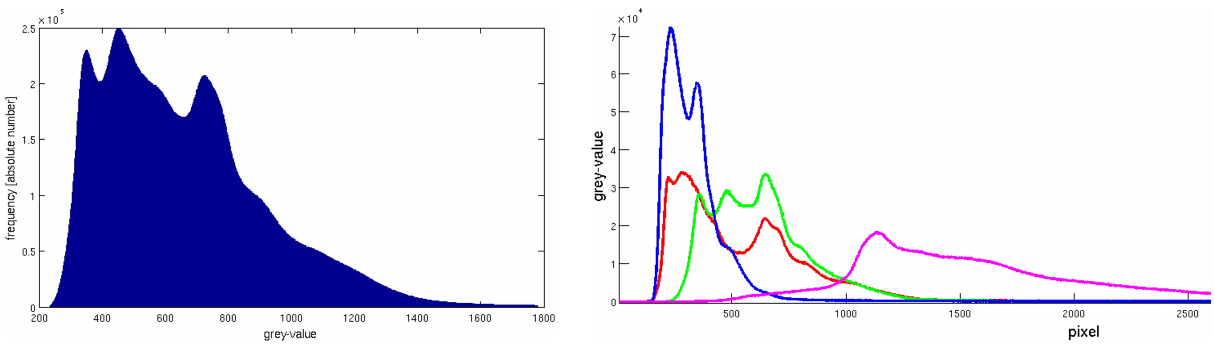

Panchromatic, level 2 RGB NIR (magenta), level 2

Fig. 7: Histogram of the UltraCamX image 10231067, radiometry dataset.

2.2 Detection of artifacts

The detection of artifacts was done visually using the original images and images with strong contrast enhancement using the Wallis filter. This enhancement allows easier visual detection of artifacts and noise. Every figure shows the flight direction using a red arrow.

2.2.1 DMC

The used DMC images are the panchromatic and the RGBNIR_8cm imagery. The pansharpened images are not further evaluated. Figure 8 shows a systematic pattern in the RGB imagery (Wallis filtered). The pattern is visible in the layer 1 (red) and 4 (NIR). The structure has a size of 11 pixels along track and 5 pixels across track. The pattern is shifted vertically one pixel after each 11 pixel wide pattern. The pattern was observed in different regions in different images. The channels G, B and PAN are not affected.

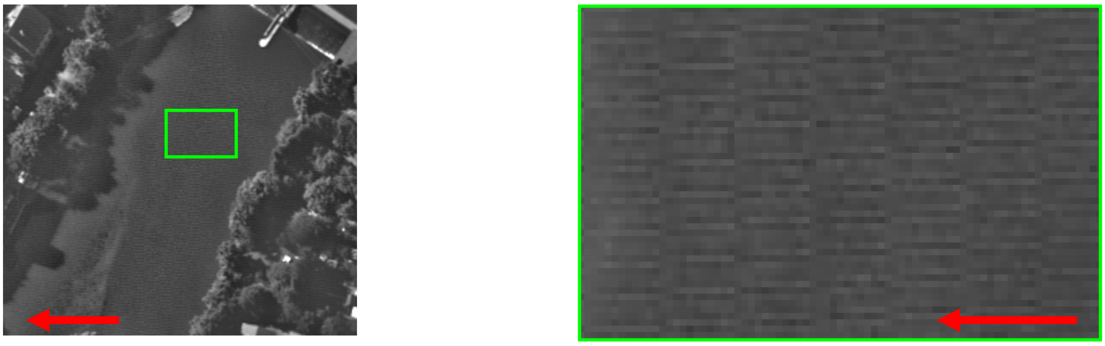

Layer 1 (red) Wallis filtered — Regular pattern in homogeneous regions

Fig. 8: DMC image 10040081.

A further pattern was detected in the panchromatic image 10040081, after Wallis filtering (Fig. 9). It shows a smearing effect along the flight direction, on the left of dark objects, as if these dark objects make subsequent pixels in the flight directions also darker.

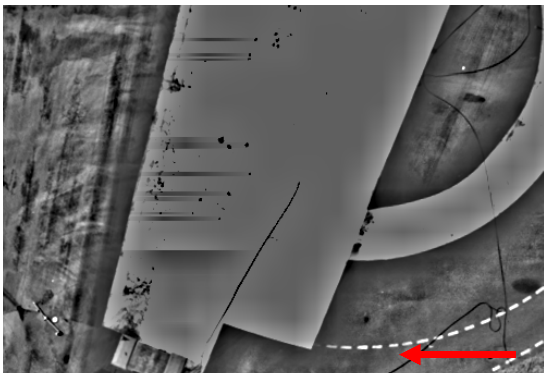

Fig. 9: DMC image 10040081, panchromatic channel, Wallis filtered.

2.2.2 ADS 40

In case of ADS 40 different datasets are available. The first one is the raw data. The second is the rectified images. Figure 10 shows the blue channel of the image 1012 (geometry dataset, raw).

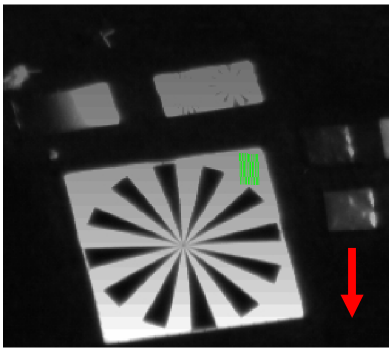

Image with profile lines

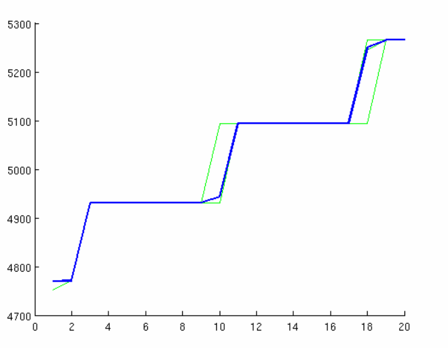

Profiles (green), average (blue)

Fig. 10: Systematic structure in the ADS 40 images, displayed using profile measurements.

In the white background of the Siemens star horizontal stripes can be noticed. The green lines (Fig. 10, left) are profiles, measured perpendicular to the detected stripes. The stripes are across the flight direction and have a width of 8 pixels. The grey levels jump from stripe to stripe by about 160 grey values.

This kind of pattern is visible in all channels of the geometry data set. It is caused by the changing compression of the images during the geometry flight, see section 2.1.2. It is visible in the panchromatic images of the radiometric block too. The color channels of the radiometric block are not affected.

A second structure occurs in saturated image areas. Fig. 11 shows this effect in the all panchromatic channels of both geometric and radiometric block (backward 14°). The pattern shows different vertical stripes with different grey values among neighbouring columns, although the area is homogeneous. This effect could not be visually detected in the spectral images. According to Leica, this happens because each line CCD pixel has a different maximum allowable grey value, which is valid for each image column. Thus, in very bright areas these stripes occur. However, Fig. 11 right shows that the profiles differ, so the previous explanation is not satisfactory. According to Leica, in between, all CCD elements have the same maximum allowable grey value, so the stripes should not occur.

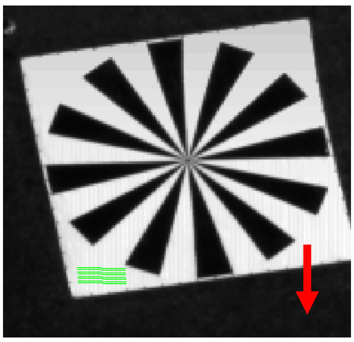

Image with profile lines

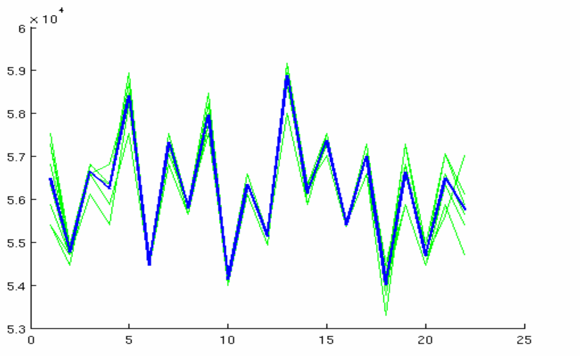

Profiles (green), average of profiles (blue)

Fig. 11: Additional pattern in the panchromatic channel, backward 14°, ADS 40.

2.3 Linearity

To estimate the linearity of the sensor, the continuous grey wedge is used. Unfortunately the area covered by this object is very small. We also did not have any reference density values for the grey wedge, while use a wedge with discrete values instead of continuous ones may be better. In addition the pattern is overexposed. Therefore, no comprehensive analysis can be made. Here, we present only first results. The following graphs show the image with the profiles (left) and the diagram (x-axis = position of pixel along the profile and y-axis = grey-value).

2.3.1 DMC

In case of the DMC, we evaluated only the panchromatic channel. The original RGB (not pansharpened) are not considered, because of the very limited size of the grey wedge in the images (few pixels). Fig. 12 shows the result of the panchromatic channel, image 10020042, geometry block. The graph shows, after a certain underexposure and a starting phase, an almost linear increasing of the grey values, starting approximately from grey value XXX and ending at the maximum grey value (saturated area).

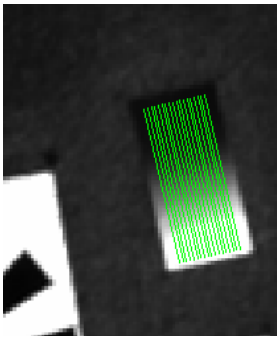

Image with profile lines

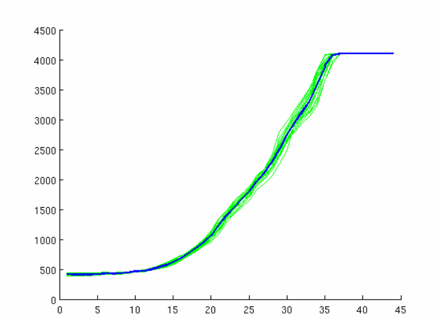

Profiles (green) and average of profiles (blue)

Fig. 12: Linearity of the DMC sensor, panchromatic image 10020042, geometry block.

2.3.2 ADS 40

Fig. 13 shows the profiles from the ADS 40, images 1_1035 of the radiometric dataset, raw.

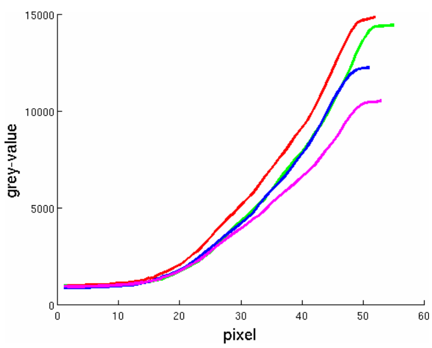

RGB and NIR (magenta)

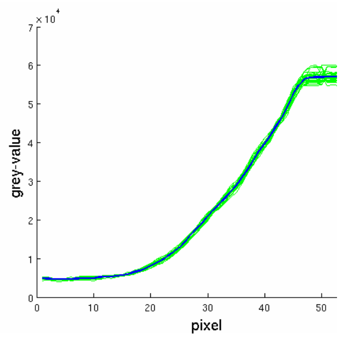

Panchromatic (backward 14°)

Fig. 13: ADS 40, radiometric block, raw, image 1_1035.

After an underexposure a linear increasing of the grey values is to observe. It ends, like in the case of DMC, in the saturated area, before the test area ends. The spectral channels show a different dynamic range among themselves with the NIR being saturated approx. at grey value 10,000, while the R channel at 15,000. They also have a lower dynamic range than the panchromatic channel. This could possibly be due to the different position of the spectral line CCDs on the focal plane compared to the panchromatic backward. Depending on the sun illumination angle, this could lead to a higher object reflectance towards the panchromatic backward CCD.

2.3.3 UltraCamX

Fig. 14 shows the profiles for the UltraCamX images. Although the images should be 12-bit, values larger than 4095 occur. The linearity of the spectral images is worse than in the other cameras, although some effects may be due to pansharpening. There are also significant differences between the spectral channels regarding dynamic range (difference between high and low saturation values). The profile for the panchromatic image is very similar to the green channel. The lowest value of the panchromatic profile (ca. 800) is higher than the corresponding value for the DMC and ADS40 (a bit less than 500), but these could well be due to different illumination and viewing angles, different sensor gain etc.

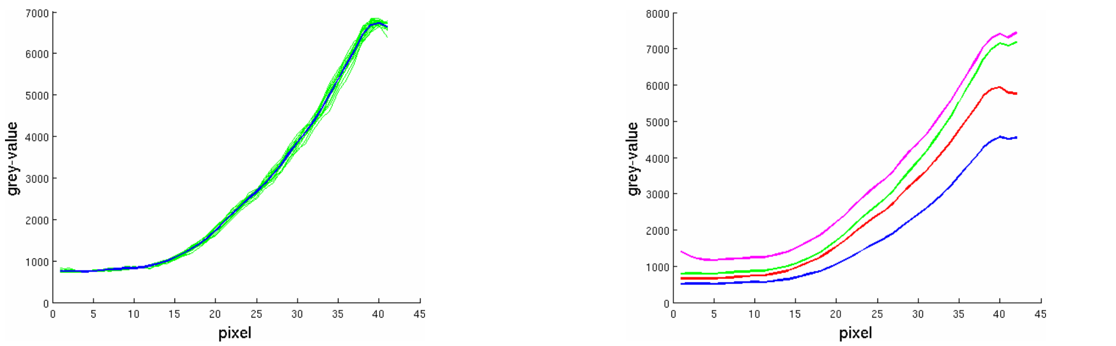

Panchromatic (level 2) RGB, NIR (magenta) (level 3 i.e. pansharpened)

Fig. 14: Profiles in the image 10231067 of the UltraCamX, radiometry block.

2.3.4 Comparison between the cameras

The following table shows the grey values where the linear part of the curves shown in Figs. 12-14 starts and ends. The start and end were determined visually. The difference between max and min grey value shows the dynamic range. A comparison of the dynamic range of the panchromatic images between the cameras should take into account the different number of bits. Doing this, ADS40 and DMC have a similar dynamic range, while UltraCamX has a much lower one. Comparing for each camera, spectral and panchromatic images, we reach the same conclusions as in the histogram analysis (i.e. for ADS40 the spectral channels have a lower dynamic range). The relation between the spectral channels is consistent with the histogram analysis for the UltraCam X, but not for the ADS40, where NIR appears to have the lowest dynamic range. In addition, it shows the length in pixels of the linear part. Since all images had the same GSD, the longer the linear part, the longer the grey wedge part is, over which linearity is achieved. For the panchromatic and spectral images the best performance is shown by ADS40. The spectral channels for each camera have similar values, and a bit better values than the panchromatic ones.

Camera	Channel	Min [grey value]	Max [grey value]	Length [pixel]
DMC	PAN	650	4095	21
ADS 40	PAN	7456	56450	28
UltraCam X	PAN	1300	6689	23
ADS 40	R	1500	14500	33
	G	1550	14400	31
	B	1650	12150	31
	NIR	1600	10500	31
UltraCam X	R	1150	5890	22
	G	1300	7200	25
	B	870	4560	22
	NIR	1500	7400	25

Table 1: Linear range of the evaluated cameras

2.4 Vignetting effects

The data was checked regarding natural vignetting of the lens by visual inspection. In the image from DMC, ADS40 and UltraCamX vignetting effects are not visible.

2.5 Interlacing detection

The datasets are tested regarding interlacing effect (differences between odd and even neighbouring columns). Therefore, the grey values of the columns are averaged line by line (as an additional test we did this also for the rows). Afterward the differences between neighbored lines are calculated. If the image contains an interlacing effect, it would be visible in the graphical visualization of the data. According to our investigations all the tested datasets are free of interlacing effects.

2.6 Noise analysis

The noise analysis was done using two visual procedures, first a Wallis filter and second a difference calculation between the original image and the same image filtered using a 3x3 local average mask. A new quantitative noise estimation method is under development.

2.6.1 DMC

According to the patchwise generation of the DMC data using 4 cameras, we tested the images regarding different noise behaviour at the four corners of the image. The used dataset does not contain any significant noise variation between the 4 cameras.

2.6.2 ADS40

Fig. 15 shows the infrared channel of the image 1012. This pattern was reproduced using the second procedure, mentioned above. The visible stripes are oriented in flight direction and seem to have a constant width. This structure is visible in both infrared channels (there were two), but not in the panchromatic and RGB images. What appears to be a problem, is just an interference effect of the monitor, which appears for a certain zoom factor. Thus, care should be taken on monitor effects when visually analyzing images.

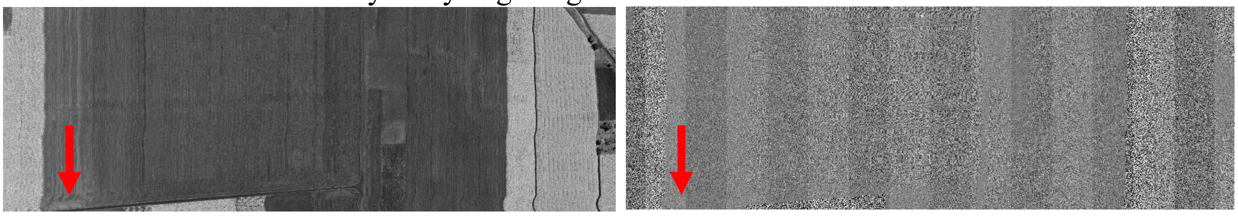

Original cut out   Structure after filtering

Fig. 15: Structure of the ADS image 1012, geometry block, raw.

2.6.3 UltraCamX

Preliminary investigations show that the UltraCamX data does not show any significant noise variations within the images but further investigations are needed.

3 Conclusions

This report shows the first results of our investigations on the radiometric behavior of the aerial cameras DMC, ADS 40 and UltraCamX. The investigations included histogram analysis, detection of artifacts, sensor linearity, vignetting and noise analysis. In some cases, there were significant problems, which may have an influence on the further image processing and generation of products (DSMs, orthoimages etc.). Several problems could not be explained up to now, but it seems that compression and sensor/electronics are major sources of errors. Further investigations and clarifications with the camera manufacturers are planned for the future.
The used test patterns were not suitable for a thorough analysis. Lack of large homogeneous areas, especially in the radiometric block made noise estimation difficult. A comparison between the cameras is very difficult due to the different image acquisition conditions (atmosphere, illumination, sensor parameters etc.). The DMC and UltraCamX images were not raw, but have been undergone an unknown processing, which has definitely altered the raw image characteristics.
Although the new digital sensor systems are providing a number of advantages in comparison to analog cameras, e.g. higher dynamic range and direct digital data acquisition, they introduce new problems, e.g. compression artifacts, that have to be considered and treated correctly during the image acquisition and processing. The digital sensors are much more complicated than the analogue ones, have frequent changes in hardware, firmware and software, which make their performance continuously changing. In addition, the camera manufactures seldom provide details on the sensors and data processing and the changes they make in their systems, thus users remain uninformed and have sometimes to use images that contain errors and influence their products. This DGPF test may contribute to an increase of information flow from the manufacturers side.